ICARUS 31, 221–243 (1977)

Global Tectonics of a Despun Planet[1]

H. JAY MELOSH

Division of Geological and Planetary Sciences, California Institute of Technology, Pasadena, California 91125

Received November 1, 1976; revised January 28, 1977

Mercury, the Moon, and many large satellites of the major planets have been tidally despun from an initially faster rotation. These bodies probably possessed equatorial bulges which relaxed as they lost their spin. An analysis of the stresses induced in an elastic shell by the relaxation of an equatorial bulge indicates that differential stresses may reach a few kilobars and that the tectonic pattern developed depends mainly upon the shell thickness. In every model studied the azimuthal stress $\sigma_{\varphi\varphi}$ is larger (more compressive) than the meridional stress $\sigma_{\theta\theta}$. For a thin elastic shell (thickness less than one-twentieth of the planet's radius) the zone from the equator to 48° latitude is characterized by strike-slip faulting. Poleward of this, normal faults and graben trending east–west are expected. Thicker elastic shells acquire an equatorial belt of thrust faults with east–west throw and rough north–south trends. These tectonic styles may be modified by a small (0.05–0.1%) radial expansion or contraction. Expansion shifts the polar normal faulting province toward the equator, while contraction shifts the equatorial provinces poleward. These patterns are not substantially altered by plastic yielding of the shell, although the equatorial thrust fault province is suppressed by strike-slip faulting until strike-slip faults occur poleward of 64.8° latitude. We conclude that there are many tectonic patterns consistent with despinning and radial contraction or expansion, but they must all be consistent with $\sigma_{\varphi\varphi} > \sigma_{\theta\theta}$. These results also indicate that the polar regions of a despun planet are of particular interest in deciding whether a given lineament system is due to stresses induced by the relaxation of the planet's equatorial bulge.

INTRODUCTION AND SUMMARY

A number of planet-sized solid bodies in the solar system have evidently lost most of their original spin angular momentum. The Moon, Mercury, Venus, Titan, and Jupiter's Galilean satellites probably had rotation periods of roughly 1 day shortly after the solar system was formed. In the process of losing their spin angular momentum, these bodies also lost some of their oblateness. This change in shape led to stresses in their (presumably) solid outer crusts, and thence to global systems of fractures if the stresses were sufficiently large. Although stresses must have locally deviated from the global pattern, a fracture network compatible with the global stress pattern might still exist in a statistical sense.

The existence of global systems of fractures or lineaments has been proposed for the Earth (Vening-Meinesz, 1947), the Moon (Fielder, 1963; Strom, 1964), Mars (Binder and McCarthy, 1972), and Mercury (Strom *et al.*, 1975; Dzurisin, 1976). Several of these investigations compare observed fracture or lineament systems with the theoretical predictions of Vening-Meinesz (1947). Unfortunately, Vening-

[1] Contribution No. 2832 of the Division of Geological and Planetary Sciences, California Institute of Technology, Pasadena, Calif. 91125.

ISSN 0019-1035

Meinesz used a rupture theory which is now known to be incorrect (Badgley, 1965). Vening-Meinesz's predicted fault patterns thus do not agree with our current understanding of the relation between faulting and stress (Anderson, 1951). Moreover, Vening-Meinesz only investigated the deformation of a thin elastic "crust" or lithosphere overlying a fluid planet. He did not consider what modifications a dense core might make, nor did he look at the effects of plastic yielding in the lithosphere.

The purpose of this paper is to reexamine the global tectonic pattern generated by a relaxed equatorial bulge in the light of a modern theory of faulting (Anderson, 1951). We also consider the effects of different lithospheric thicknesses, the presence of a core (or other density discontinuities), and plastic yielding of the lithosphere.

We find that the stress pattern due to a relaxed equatorial bulge is not very sensitive to the internal structure of the despun body, although the actual magnitude of the stress is dependent upon lithospheric thickness. The azimuthal stress $\sigma_{\varphi\varphi}$ always exceeds the meridional stress $\sigma_{\theta\theta}$ except at the poles, where they are equal. The azimuthal stress $\sigma_{\varphi\varphi}$ is generally compressive from the equator to about 40° latitude, poleward of which it becomes tensional. The sign of $\sigma_{\theta\theta}$ is more dependent upon details of internal structure, particularly upon lithospheric thickness.

The system of fractures resulting from this stress system includes three distinct provinces (Fig. 1). There is an equatorial province, extending from about 30°S latitude to 30°N or less, depending upon lithospheric thickness. Thrust faults are expected to form in this province. These faults form in response to dominant azimuthal compression, and so should have east–west throws with roughly north–south trends.

Right lateral strike-slip faults trending roughly N 60°E and left lateral strike-slip

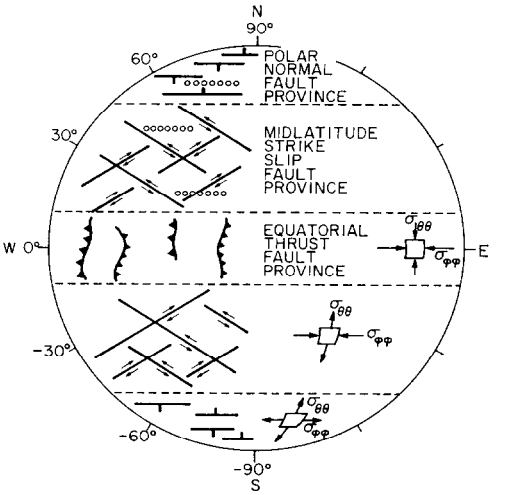

FIG. 1. Schematic representation of the stresses and associated faulting in the three tectonic provinces which can occur on a despun planet. These stresses are a consequence of the relaxation of the planet's equatorial bulge. The rows of small circles in the strike-slip and normal faulting provinces indicate alignments of volcanic craters and represent the fact that dike injection proceeds perpendicular to the least principal axis. Vertical dikes controlled by the global stress pattern should thus strike east and west.

faults trending N 60°W form in a latitudinal zone extending from 30 or less to about 50°. The extent of this province depends strongly upon lithospheric thickness. If the thickness of the lithosphere is between one-half and one-tenth of the planet's radius, then the zone of strike-slip faulting may cover only about 15° of latitude. On the other hand, if the lithosphere is thinner than one-twentieth of the planet's radius, there will be no thrust faulting at all, and strike-slip faults will extend from the equator to 48° latitude.

The regions poleward of about 40° latitude are provinces of tensional stress [this was noted by Burns (1976), who used Vening-Meinesz's solutions and thus placed the boundary at 55° latitude]. The nature of faulting in this province depends upon depth in the lithosphere. Thus, in the near-surface region (the upper few kilometers)

brittle failure of rocks in tension should produce joints trending east–west. There may be a transitional region between the midlatitude shear fractures and the polar east–west tension fractures, where the 60° opening angle between conjugate shears closes to zero (Brace, 1964). Deeper in the lithosphere, lithostatic pressure is large enough to ensure that no principal stress is tensional. In this case, the minimum principal stress is meridional (north–south), while the maximum stress is vertical. We thus expect graben trending east–west. These graben may be cut by north–south cross joints once the primary meridional tension has been relieved. We do not know enough about the response of lithospheric material to tensional forces to say which depth will dominate. It is possible that the result will be a superposition of fracture patterns developed at both near-surface and deeper levels (deep fractures thus propagating upward to the surface). In either case, however, the extensional stresses in the polar provinces lead us to expect strong east–west lineaments.

The fact that such polar east–west lineaments have not been observed on either the Moon (Strom, 1964, and personal communication, 1976) or Mercury (Dzurisin, 1976) seems to argue against the hypothesis that the fracture systems on these planets are due to despinning and consequent relaxation of an equatorial bulge. We note, however, that the tensional or compressional provinces may be extended to any degree desired if the planet is allowed either to expand or to contract radially while it is being despun.

Purely radial expansion leads to tensional $\sigma_{\theta\theta}$ and $\sigma_{\varphi\varphi}$ which are equal over the whole planet. Superimposed on the stress field due to despinning, its effect is to bring the polar tensional province closer to the equator. For a sufficiently large expansion (still less than a few tenths of 1% of the planet's radius) the tensional tectonic province can cover the entire planet. Conversely, radial contraction leads to equal compressional $\sigma_{\theta\theta}$ and $\sigma_{\varphi\varphi}$ and may thus act to extend the equatorial thrust faulting province to the poles. Figure 5 shows how radial expansion or contraction affects the extent of the three tectonic provinces.

A combination of stresses due to despinning and expansion or contraction may thus be used to explain a variety of global fracture patterns. No combination of these stress systems, however, could explain features due to north–south compression or east–west tension. Thus, conjugate shear fractures whose acute angle is bisected by a north–south line, or north–south-trending graben are outside the scope of this analysis. If strong evidence of such features is found, then we cannot postulate that the stresses which produced them were due to despinning.

In the following pages we show how these conclusions come about in more detail. The more intimate details of the stress field in an elastic shell are relegated to the Appendix. In the text we concentrate upon a few simple examples of the more general calculations.

STRESSES ACTING IN A DESPUN PLANET

A nonrotating, self-gravitating mass of fluid tends to assume a spherical shape in the absence of other forces. If it rotates slowly, then the stable configuration is an oblate, or flattened, spheroid. Contours of equal pressure in such a body coincide with equipotential surfaces in the rotating system, and no deviatoric or shear stresses are present. The equation describing the surface of a slowly rotating mass in hydrostatic equilibrium is

$$r = a[1 - (f/6)(1 - 3\cos 2\lambda)], \quad (1)$$

where r is the radial distance from the center of the spheroid to the surface, a is its mean radius, λ is the latitude, and f is the spheroid's flattening, defined as

$$f = (r_{\text{equatorial}} - r_{\text{polar}})/a. \quad (2)$$

There are two terms in the gravitational potential which contribute to the departure of equipotential surfaces from perfect sphericity. The first is the "centripetal potential" $U_c = \frac{1}{2}\omega^2 r^2 \cos^2 \lambda$, where ω is the angular velocity of rotation. This term arises from the fact that we seek equilibrium in a rotating coordinate system. The other term comes from the deformed mass itself: an oblate spheroidal mass generates an oblate gravitational field. When both terms are added and we require that surfaces of constant pressure within the mass are equipotential surfaces, an equation for the surface flattening results. The solution to this equation is well known (Jeffries, 1952):

$$f = \frac{\frac{5}{2}m}{1 + \{\frac{5}{2}[1 - \frac{3}{2}(C/Ma^2)]\}^2}. \quad (3)$$

In this equation

$$m = \frac{\text{centripetal acceleration at equator}}{\text{gravitational acceleration}} = \frac{\omega^2 a^2}{GM}, \quad (4)$$

where G is the gravitational constant and M is the bodies' mass. The condition of "slow rotation" means that m must be much smaller than 1. The quantity C in (3) is the polar moment of inertia. For the purposes of this paper, no great error will result if we assume the body has uniform density, in which case we can take

$$f = (5/4)m \quad \text{(uniform density)}. \quad (5)$$

Thus, if Mercury were in hydrostatic equilibrium and had a period of 20 hr this formula predicts a flattening $f = 1/160$, somewhat larger than the value of 1/298.25 for the Earth.

In the following work, we assume that the planetary body in question originally began in a state of hydrostatic equilibrium with flattening given by (5). The model thus assumes that there were no deviatoric stresses in the body before it began to lose its spin. This does not appear unreasonable in the light of evidence for early differentiation of virtually all planet-sized bodies in the solar system. During the differentiation process, the entire planet was probably hot enough to eliminate stress differences by viscous flow or creep. Later, when a brittle lithosphere formed by surface cooling, stress differences could be supported elastically.

After the formation of an elastic lithosphere, the planet lost some fraction of its spin, decreasing m to m'. At the same time, the flattening decreased from $f = (5/4)m$ to f'. If the new flattening f' was equal to $(5/4)m'$, we would again have a hydrostatic stress state with no shear stresses. This would be the case for a fluid sphere. However, an elastic sphere, or a planet with a fluid interior and an elastic lithosphere, resists changes in shape. The nonhydrostatic stresses which develop in the elastic portion of the planet tend to make f' larger than $(5/4)m'$. If these stresses become large enough, rupture can occur, thus relieving stress and decreasing f' toward the hydrostatic value. The relation between the change in rotation rate (i.e., $m - m'$) and the stress developed in the elastic portion of the planet is a function of the planet's internal structure.

We explore a range of models which should encompass all of the possibilities actually occurring in the solar system. In this work we use Mercury for numerical examples, although the actual results are more general. Most of the details of this work are in the Appendix. However, to give the reader a general idea of the method, we describe two of the simpler limits in more detail. We then go on to discuss the results of more general computations.

Example: Despinning of an Incompressible Elastic Spheroid

In the initial, hydrostatic configuration with flattening f and rotational parameter m the gravitational potential inside an oblate spheroid of uniform density ρ and

mass M is (Jeffries, 1952)

$$U = -\frac{GM}{a}\left[\frac{3a^2 - r^2}{2a^2} + \frac{m}{3}\frac{r^2}{a^2} - \frac{1}{2}\left(\frac{f}{5} + \frac{m}{6}\right)\frac{r^2}{a^2}(1 - 3\cos 2\lambda)\right], \quad (6)$$

where G is Newton's gravitational constant.

Equilibrium of forces requires

$$\nabla p(r, \lambda) = -\rho \nabla U, \quad (7)$$

where $p(r, \lambda)$ is pressure. The solution to this equation is

$$p(r, \lambda) = \text{constant} - \rho U. \quad (8)$$

The constant is determined by the requirement that $p(r, \lambda) = 0$ on the oblate surface (1). In general, a suitable constant for (8) can only be found if $f = (5/4)m$. When this is the case, we find

$$p(r, \lambda) = \frac{\rho GM}{a}\left[\frac{a^2 - r^2}{2a^2} - \frac{4}{15}f\left(1 - \frac{r^2}{a^2}\right) - \frac{f}{6}\frac{r^2}{a^2}(1 - 3\cos 2\lambda)\right], \quad (9)$$

and the stress tensor σ_{ij} is given by

$$\begin{aligned} \sigma_{rr} &= \sigma_{\theta\theta} = \sigma_{\varphi\varphi} = p(r, \lambda), \\ \sigma_{r\theta} &= \sigma_{r\varphi} = \sigma_{\theta\varphi} = 0. \end{aligned} \quad (10)$$

Note that compressive stress is positive. Figure 2 illustrates the coordinate system. The reader may easily check that (9) satisfies $p(r, \lambda) = 0$ on the oblate surface (1) to first order in f (we neglect terms of order f^2 and mf).

Suppose m decreases to m'. The flattening of the spheroid decreases to f' and the new surface is given by

$$r' = a[1 - (f'/6)(1 - 3\cos 2\lambda)]. \quad (11)$$

The internal gravitational potential becomes

$$U' = -\frac{GM}{a}\left[\frac{3a^2 - r^2}{2a^2} + \frac{m'}{3}\frac{r^2}{a^2} - \frac{1}{2}\left(\frac{f'}{5} + \frac{m'}{6}\right)\frac{r^2}{a^2}(1 - 3\cos 2\lambda)\right]. \quad (12)$$

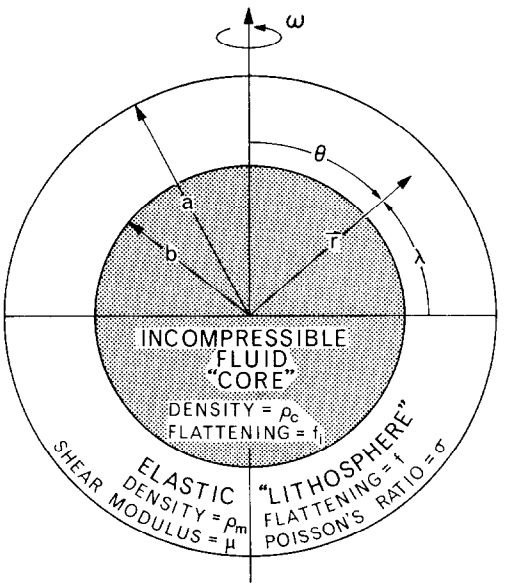

FIG. 2. Geometry of the despun planet and definition of several variables. The planet is modeled as an elastic shell or lithosphere with external radius a, internal radius b, overlying an incompressible fluid core of density ρ_c. The lithosphere is described by its shear modulus μ, density ρ_m, and Poisson's ratio σ. The flattening, defined as the difference between the equatorial and polar radii divided by the mean radius, is f for the outer surface of the elastic shell, and f_i for its interior. The latitude of a point within the planet is given by λ, its colatitude is θ, and its distance from the center is r. The planet spins with an angular velocity ω.

The pressure can be computed as before. Evaluating this pressure on the surface (11) we find

$$p'(\text{surface}') = \text{constant}' + \frac{\rho GM}{a}\left[\frac{1}{15}\left(f' - \frac{5}{4}m'\right) \times (1 - 3\cos 2\lambda)\right]. \quad (13)$$

Thus, unless $f' = (5/4)m'$ (the hydrostatic value) we cannot obtain zero pressure on the surface at all latitudes. However, the boundary conditions at the free surface of a body require

$$\begin{aligned} \sigma_{rr} &= p'(\text{surface}') = 0, \\ \sigma_{r\theta} &= 0. \end{aligned} \quad (14a)$$

Obviously, a stress component σ_{rr} must be added from some other source. The source of this extra stress is the elastic deformation of the spheroid. The surface of the spheroid has been displaced radially by an amount

$$u_r = r - r' = -(a/6)(f - f') \times (1 - 3\cos 2\lambda). \quad (15)$$

The stress equilibrium equations for an incompressible elastic sphere admit only two solutions for a surface deformation of type (15) [see Jeffries (1952) and Appendix]: These solutions imply

$$\begin{aligned} u_r &= (\alpha r + \beta r^3)(1 - 3\cos 2\lambda), \\ \sigma_{rr}^{el} &= \mu(2\alpha - \beta r^2)(1 - 3\cos 2\lambda), \\ \sigma_{r\theta}^{el} &= -2\mu(3\alpha + 8\beta r^2)\sin 2\lambda, \end{aligned} \quad (16)$$

where μ is the shear modulus of the planet and α and β are constants which are to be determined; these constants describe the amount of stress contributed by each of the two solutions. The boundary conditions (14a) thus become

$$\begin{aligned} \sigma_{rr}^{el}(a, \lambda) + p'(\text{surface}') &= 0, \\ \sigma_{r\theta}^{el}(a, \lambda) &= 0 \end{aligned} \quad (14b)$$

(note that σ_{ij}^{el} are already of order f so that we may evaluate them at $r = a$ to sufficient accuracy). The application of these boundary conditions determines α and β, yielding the result

$$f - f' = \frac{(5/4)(m - m')}{1 + (19/2)(a\mu/\rho GM)}. \quad (17)$$

Note the important role of the dimensionless constant

$$\frac{1}{2}\frac{a\mu}{\rho GM} = \left(\frac{\nu_s}{\nu_e}\right)^2 = \left(\frac{\text{shear wave velocity in planet}}{\text{escape velocity of planet}}\right)^2. \quad (18)$$

If this constant is much smaller than 1, as for a large massive planet, (17) shows that $(f - f') \simeq (5/4)(m - m')$. Thus, f' never departs much from the hydrostatic value $(5/4)m'$. The planet is not strong enough to support a large nonhydrostatic bulge, although elastic stresses do build up in the interior.

If the constant (18) is much larger than 1, as for a small planet, f' will not differ much from f, $(f - f') \simeq 0$. In this case the strength of the planet is sufficient to maintain the nonhydrostatic bulge against the forces tending to relax it. The equatorial bulge acts like a load applied to the surface of an elastic spheroid.

Unfortunately, the shear wave velocities of the terrestrial planets are comparable to their escape velocities. Thus, for the Moon, $(\nu_s/\nu_e)^2 \cong 2.8$, for the Earth it is 0.16, and if Mercury has the same shear wave velocity as the Earth (about 4.5 km/sec in the upper mantle), $(\nu_s/\nu_e)^2 \cong 1.1$ for Mercury. We thus cannot approximate (17) by one of its limits for the terrestrial planets.

The boundary conditions (14b) determine α and β. The entire stress field thus becomes known. Near the surface $\sigma_{\theta\theta}^{el}$ and $\sigma_{\varphi\varphi}^{el}$ are

$$\begin{aligned} \sigma_{\theta\theta}^{el}(a, \lambda) &= -\frac{\mu(f - f')}{30}(31 - 57\cos 2\lambda), \\ \sigma_{\varphi\varphi}^{el}(a, \lambda) &= -\frac{\mu(f - f')}{30}(13 - 75\cos 2\lambda). \end{aligned} \quad (19)$$

The total stresses $\sigma_{\theta\theta}$ and $\sigma_{\varphi\varphi}$ may be obtained from the elastic stresses $\sigma_{\theta\theta}^{el}$ and $\sigma_{\varphi\varphi}^{el}$ by adding the pressure p to the elastic stresses.

$$\begin{aligned} \sigma_{rr}(\text{surface}') &= \sigma_{rr}^{el} + p'(\text{surface}') = 0, \\ \sigma_{\theta\theta}(\text{surface}') &= \sigma_{\theta\theta}^{el} + p'(\text{surface}') \\ &= -\tfrac{2}{5}\mu(f - f'), \\ \sigma_{\varphi\varphi}(\text{surface}') &= \sigma_{\varphi\varphi}^{el} + p'(\text{surface}') \\ &= \tfrac{1}{5}\mu(f - f')(1 + 3\cos 2\lambda). \end{aligned} \quad (20)$$

At the poles, $\lambda = \pm 90°$,

$$\sigma_{\theta\theta} = \sigma_{\varphi\varphi} = -\tfrac{2}{5}\mu(f - f')$$

so both $\sigma_{\theta\theta}$ and $\sigma_{\varphi\varphi}$ are tensional. The difference between the azimuthal and meridional stresses is always positive,

$$\sigma_{\varphi\varphi}(a, \lambda) - \sigma_{\theta\theta}(a, \lambda) = \tfrac{3}{5}\mu(f - f')(1 + \cos 2\lambda); \quad (21)$$

hence $\sigma_{\varphi\varphi}$ is always larger than $\sigma_{\theta\theta}$. The maximum difference (at the surface) occurs on the equator where

$$\sigma_{\varphi\varphi} - \sigma_{\theta\theta} = (6/5)\,\mu(f - f').$$

The azimuthal stress $\sigma_{\varphi\varphi}$ is compressive up to 55° latitude, poleward of which it becomes tensional. The meridional stress $\sigma_{\theta\theta}$ is tensional at all latitudes. The general stress pattern is thus exactly as described in the Introduction, and the tectonic provinces follow that pattern.

An estimate of the size of $\mu(f - f')$, and thus of the maximum stress differences, can be easily made for a body of the size and mass of Mercury. Taking $f = 1/160$ originally, and supposing the rotation to be completely stopped, $m' = 0$, we find (using $\mu = 6.5 \times 10^{11}$ dyn/cm^2) that $f' = 1/173$ (nearly the same as f) and that $\mu(f - f') \simeq 300$ bars. This stress is comparable with that associated with deviations from isostasy in both the Earth and the Moon. However, it seems unlikely that major fracturing of the Mercurian lithosphere would result from such stress differences.

Thus, if Mercury (or smaller bodies, such as the Moon) can be accurately modeled as incompressible elastic spheroids, we expect that they are capable of supporting large nonhydrostatic bulges. In fact, Mercury does not have any detectable flattening (Howard *et al.*, 1974), suggesting that this model is inadequate. The obvious modification is to suppose that Mercury is better described by an elastic shell with a fluid interior. In this case the factor $(\nu_s/\nu_e)^2$ in (18) is multiplied by a term of order t/a, where t is the thickness of the elastic shell. Thus for a sufficiently thin shell the flattening remains near the hydrostatic value of $(5/4)m'$, even though large stresses may build up in the shell.

When we speak of a "fluid" interior to the elastic shell, we do not necessarily mean a liquid interior. All that is required of the interior is that it does not support stress differences over a period of time comparable to the spindown time of the planet. This is equivalent to insisting that the Maxwell relaxation time $\tau = \eta/\mu$ (where η is the effective viscosity of the material) be shorter than the spindown time in the "fluid" interior, but longer than the spindown time in the "elastic" shell. The thickness of the "elastic" shell is thus determined by the rheology of the planet's interior. In particular, this shell need not coincide with any compositional or phase boundary in the planet.

The detailed solutions for stress developed in a planet with an elastic shell of a given thickness are presented graphically in Fig. 3. These solutions are algebraically messy and are discussed in the Appendix. In the next section we discuss the logical limit of a very thin shell.

Example: Despinning of a Planet with a Thin Elastic Lithosphere

A very thin elastic shell or lithosphere cannot exert appreciable bending stress and so cannot support a nonhydrostatic equatorial bulge. Thus, for a sufficiently thin lithosphere the flattening is nearly equal to the hydrostatic value,

$$f' \cong (5/4)m' \qquad \text{(thin lithosphere)}. \quad (22)$$

Even though the lithosphere cannot exert bending moments, it does develop stresses due to stretching. These stresses can be evaluated either by taking the $t \to 0$ limit of the stress in an elastic shell (see Appendix), or by rewriting the equilibrium equations in such a way as to drop the bending terms (Vening-Meinesz, 1947). In either

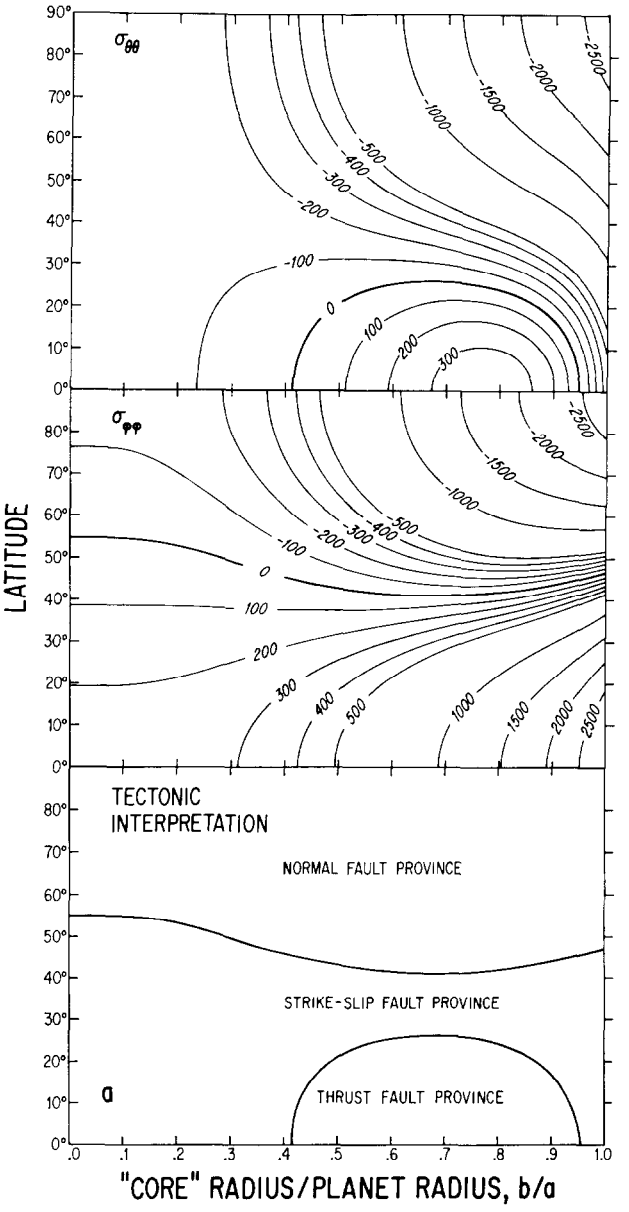

FIG. 3. Dependence of the stress and tectonic style of a despun planet on lithospheric thickness and the insensitivity of the stress pattern to the presence of a dense core or compressibility of the lithosphere. Each plot summarizes the stress developed in an array of model planets. The vertical axis is latitude on the planet, and the horizontal axis is the ratio between the core radius and the planet's radius, b/a. Thus, for a solid elastic sphere $b/a = 0$ while for an infinitesimally thin lithospheric shell $b/a = 1$. The contours represent the stress in bars developed in a planet with a given b/a ratio at various latitudes. The way to read the plots is to choose a value of b/a for some particular model, draw a vertical line, and read off the latitudes at which the stress equals the contour value. The top plot in each sequence is the meridional stress $\sigma_{\theta\theta}$, the middle plot is the azimuthal stress $\sigma_{\varphi\varphi}$, and the bottom plot is the tectonic interpretation of these two

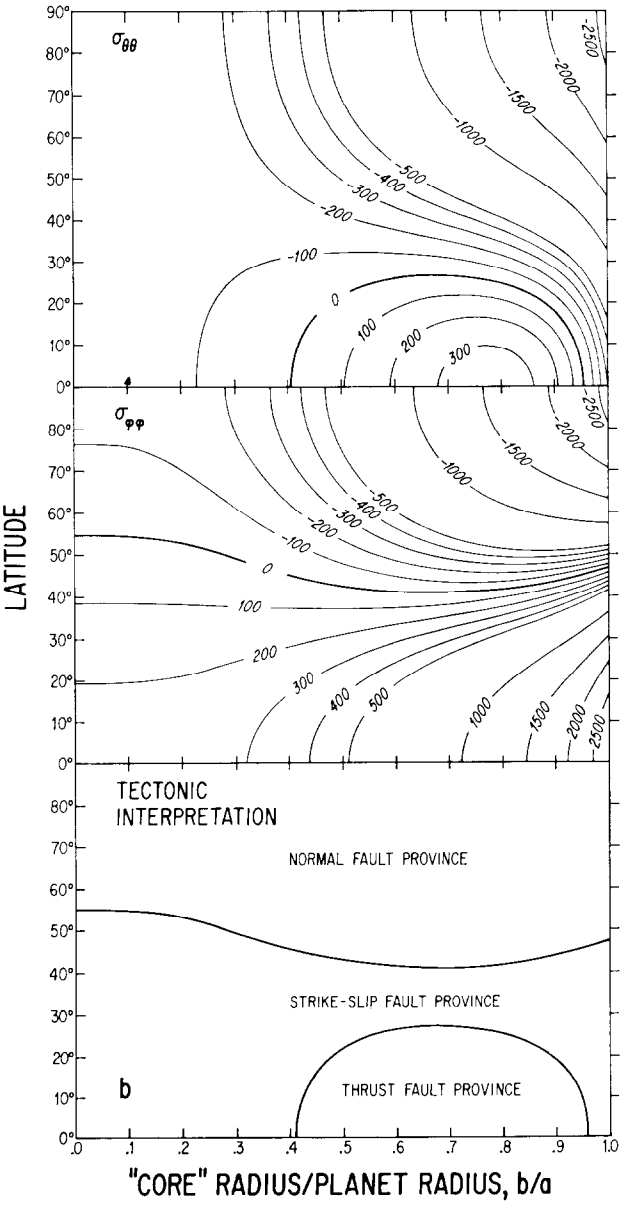

stress fields. Since $\sigma_{\theta\theta}$ and $\sigma_{\varphi\varphi}$ are horizontal stresses at the surface, $\sigma_{rr} = 0$. The parameters used to compute the stress contours were chosen to approximate the conditions of Mercury. The initial period was 20 hr; the final period, 1400 hr (59 days); the radius of the planet, 2439 km; the mean density, 5.44 g/cm^3; and the shear modulus, 6.5×10^{11} dyn/cm^2. Figure 3a was computed for a lithosphere with Poisson's ratio $\sigma = 0.5$ (incompressible), and the ratio of core density to lithosphere density $\rho_c/\rho_m = 1$. Figure 3b was computed for $\sigma = 0.5$ as before, but with $\rho_c/\rho_m = 2$. We see that the presence of a dense core has very little influence on the surface stress pattern. Figure 3c examines the effect of compressibility: $\sigma = 0.25$ and $\rho_c/\rho_m = 1$. Again, it is evident that the stress pattern is not very dependent upon compressibility.

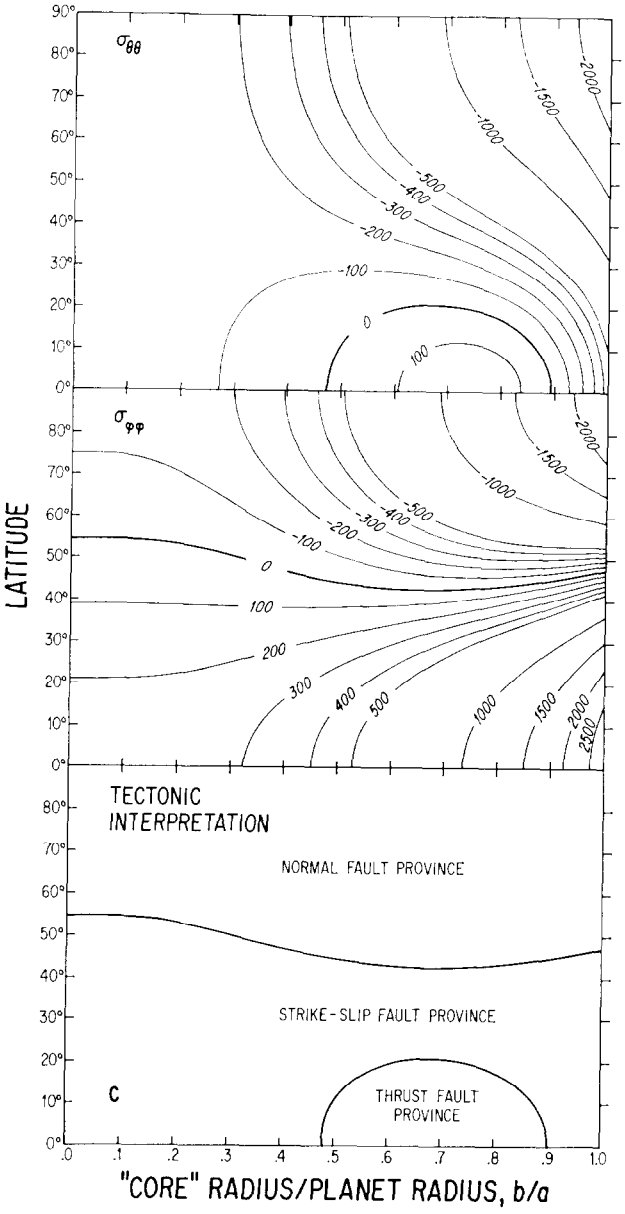

FIG. 3—*Continued*

case the same equations result:

$$u_r = -\frac{5}{24}a(m - m')(1 - 3\cos 2\lambda),$$

$$\sigma_{\theta\theta} = -\frac{5}{12}(m - m')\mu\left(\frac{1 + \sigma}{5 + \sigma}\right) \times (5 - 3\cos 2\lambda), \tag{23}$$

$$\sigma_{\varphi\varphi} = \frac{5}{12}(m - m')\mu\left(\frac{1 + \sigma}{5 + \sigma}\right) \times (1 + 9\cos 2\lambda),$$

where σ is Poisson's ratio for the elastic material of the lithosphere. We see that the difference $\sigma_{\varphi\varphi} - \sigma_{\theta\theta}$ is positive at all

latitudes,

$$\sigma_{\varphi\varphi} - \sigma_{\theta\theta} = \tfrac{5}{2}(m - m')\mu\left(\frac{1+\sigma}{5+\sigma}\right) \times (1 + \cos 2\lambda), \quad (24)$$

so that $\sigma_{\varphi\varphi} > \sigma_{\theta\theta}$ at all latitudes for a thin lithosphere as well as for a solid elastic spheroid. The maximum stress difference again occurs at the equator, where $\sigma_{\varphi\varphi} - \sigma_{\theta\theta} = 5(m - m')\,\mu(1 + \sigma)/(5 + \sigma)$. The azimuthal stress $\sigma_{\varphi\varphi}$ is compressive up to 48° latitude, poleward of which it becomes tensional. The meridional stress $\sigma_{\theta\theta}$ is tensional at all latitudes. The stress pattern is thus generally similar to that of a solid elastic spheroid. The major difference between the stress field (23) for a thin crust and the stress field (20) for a solid spheroid is the magnitude of the stresses. If Mercury originally had $f = 1/160$ ($m = 0.0050$) and m' was reduced to zero, then the maximum stress difference in a thin lithosphere is of order $(m - m')\,\mu = 3260$ bars ($\mu = 6.5 \times 10^{11}$ dyn/cm^2). This stress difference is about ten times larger than the maximum stress difference in a solid elastic spheroid. It far exceeds the average stress differences present in the lithosphere of the Earth or the Moon and there seems little doubt that it is sufficient to rupture the lithosphere of Mercury. If the Mercurian global fracture system is to be explained in terms of a relaxed equatorial bulge, it is thus necessary for Mercury to behave as if it consisted of a thin elastic shell overlying a fluid interior.

The General Problem

Figure 3 presents the results of a suite of models. Since the normal component of stress σ_{rr} is zero at the surface of the planet, we plot only the azimuthal stress $\sigma_{\varphi\varphi}$ and the meridional stress $\sigma_{\theta\theta}$. The value of each stress component is determined over a range of latitudes from 0 to 90° and for some value of the ratio of the shell thickness to the planet's radius. Figure 3 shows contours of $\sigma_{\varphi\varphi}$ and $\sigma_{\theta\theta}$ on a plot of latitude versus this ratio. The numerical values of the stresses in Fig. 3 are derived with reference to Mercury. Thus, we have assumed that the planet's initial hydrostatic flattening was $f = 1/160$ and that it was completely despun ($m' = 0$). We have taken the constant (18) $(\nu_s/\nu_c)^2 = 1.1$ and $\mu = 6.5 \times 10^{11}$ dyn/cm^2. The stress values are proportional to $(m - m')$. The change in flattening $(f - f')$ is plotted as a function of shell thickness in Fig. 4 for the three different cases shown in Figs. 3a, b, and c.

Figure 3a displays the stresses $\sigma_{\theta\theta}$ and $\sigma_{\varphi\varphi}$ developed on the surface of an incompressible elastic shell as a result of despinning. The density of the planet is assumed to be uniform. Figure 3a also includes a tectonic interpretation of the stress pattern, to be discussed more thoroughly in the next section. Figure 3b is a similar plot of the stresses developed on the surface of an incompressible elastic shell whose interior is filled with a fluid twice as dense as the shell. The density difference between the shell and the fluid causes stress to be exerted on the interior of the shell, thus altering its elastic response. Figure 3c displays the effect of compressibility, where the stresses developed in an elastic shell with Poisson's ratio $\sigma = 0.25$ on a planet of uniform density are computed.

The most notable feature of Figs. 3a, b, and c is their similarity. Although there are differences in detail, the overall stress patterns are nearly identical. The lesson we learn is that neither the presence nor the absence of a dense core or varying degree of compressibility can affect the stress patterns due to despinning.

Lithospheric thickness is the dominant factor in regulating both the magnitudes of the stresses and their patterns. In general, the thinner the lithosphere, the larger the stresses and stress differences become. Moreover, a planet with a lithosphere thicker than about one-twentieth of the planet's radius and thinner than one-half

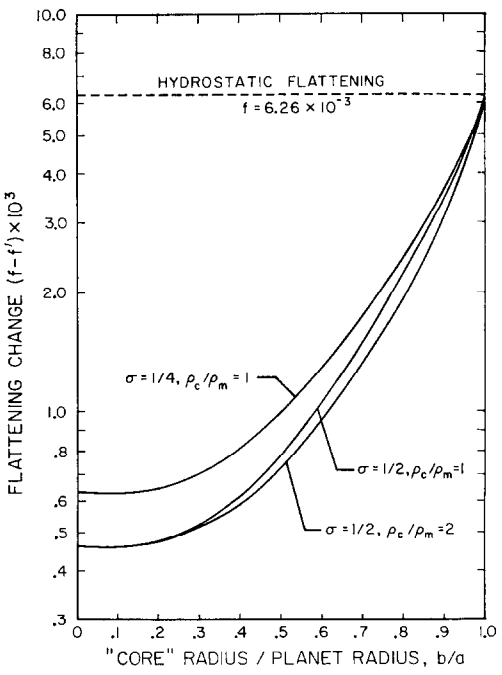

FIG. 4. The difference between the final flattening f' of a despun planet and its initial, hydrostatic value f, for a variety of model planets. When the planet has a very thin elastic lithosphere, $b/a = 1$, the difference $f - f'$ is equal to f; i.e., the flattening of the despun planet is zero, and it cannot support any equatorial bulge. If the planet is modeled as a solid elastic sphere, $b/a = 0$, it can evidently support a considerable equatorial bulge ($f - f' \neq f$). The curves show the results for intermediate cases. The three curves are computed for the models described in Fig. 3a, b, and c. The corresponding surface stresses may be found from Fig. 3.

the radius will have an equatorial zone in which both $\sigma_{\theta\theta}$ and $\sigma_{\varphi\varphi}$ are compressive. If the lithosphere is thinner than about one-twentieth of the planet's radius, this zone disappears and $\sigma_{\theta\theta}$ is tensional from equator to pole.

Before discussing the effects of these stress fields on crustal tectonics, we note that the character of the stresses induced by despinning can be greatly altered if the planet expands or contracts slightly as it despins. Such radial motions may be due to heating or cooling of the planet's interior or to phase transformations taking place at constant temperature. A certain amount of contraction is due to despinning itself, since (9) shows that the average pressure at any depth is a function of the spin. As the planet despins the average pressure increases, compressing the interior. [Stoneley (1924) has shown that the stress due to this compression is small in comparison to the stress due to the change in oblateness for the Earth.]

The stress developed near the surface of a planet whose radius has decreased by an amount Δ is given by

$$\sigma_{\theta\theta}(a) = \sigma_{\varphi\varphi}(a) = 2\mu \frac{1 + \sigma}{1 - \sigma} \frac{\Delta}{a},$$
$$\sigma_{rr}(a) = 0. \tag{25}$$

The thickness of the elastic shell does not affect the stress. This equation shows that a 1% contraction generates compressive stresses of tens of kilobars.

Superposition of stress fields due to despinning and to expansion or contraction yields a wide range of tectonic models. The various tectonic provinces can be shifted, extended or reduced by different amounts of radial motion (see Fig. 5). The one constant factor in all of these models is that $\sigma_{\varphi\varphi} > \sigma_{\theta\theta}$. This relation holds for all stress fields due to despinning. Since contraction or expansion produces equal $\sigma_{\theta\theta}$ and $\sigma_{\varphi\varphi}$, the superposition of these two processes preserves $\sigma_{\varphi\varphi} > \sigma_{\theta\theta}$.

Now that we understand the nature of the elastic stresses generated by despinning and expansion or contraction of a planet, we go on to describe the implications of these stresses for crustal tectonics. We also investigate the modification introduced by plastic yielding of the crust.

THE RELATION BETWEEN STRESS AND TECTONICS

The modern view of the relation between faulting and stress is expounded at some length by Anderson (1951). In brief, Anderson proposes that all faults are shear

fractures. The plane of failure lies at an angle of about 30° to the direction of maximum compressive stress and includes the intermediate stress axis. Rock mechanics investigations confirm the 30° angle and indicate that the failure stress depends upon ambient pressure as well as the difference between the maximum and minimum principal stresses (Handin, 1966).

Near the surface of a planet stress boundary conditions require that one of the principal stresses be perpendicular to the surface. Since there are three principal stresses, there are three orientations of the shear failure plane and thus three styles of faulting are possible. Depending upon whether the maximum, intermediate, or minimum principal stress is perpendicular to the surface we expect normal faults, strike-slip faults, or thrust faults. The orientation of the stresses acting horizontally in the planet's crust determines the orientation of faults observed.

For a despun planet we have found that $\sigma_{\varphi\varphi} > \sigma_{\theta\theta}$ and $\sigma_{rr} = 0$ near the surface. Contraction or expansion of the planet contributes equally to the $\sigma_{\varphi\varphi}$ and $\sigma_{\theta\theta}$ components, but does not alter σ_{rr}. The addition of a hydrostatic pressure, as occurs with increasing depth in the planet, does not alter the principal stress orientation since it contributes equally to all stress components

$$\sigma_{rr} = \sigma_{\theta\theta} = \sigma_{\varphi\varphi} = \rho g(a - r) \quad \text{(hydrostatic)}, \quad (26)$$

where g is the surface gravity (360 cm/sec^2 for Mercury, giving a vertical pressure gradient of 110 bars/km for a crustal density of 3 g/cm^3). These simple principles allow us to distinguish three tectonic provinces on the planet:

1. Equatorial zone of thrust faulting. $\sigma_{\varphi\varphi} > \sigma_{\theta\theta} > \sigma_{rr}$. When $\sigma_{\varphi\varphi}$ and $\sigma_{\theta\theta}$ are both compressive they exceed $\sigma_{rr} = 0$. The minimum principal stresses is thus vertical, so that thrust faults are expected. Since $\sigma_{\varphi\varphi} > \sigma_{\theta\theta}$, displacement will be east–west and the faults will trend roughly north–south.

2. Equatorial to midlatitude zone of strike-slip faults. $\sigma_{\varphi\varphi} > \sigma_{rr} > \sigma_{\theta\theta}$. If $\sigma_{\varphi\varphi}$ is compressive and $\sigma_{\theta\theta}$ is tensional, σ_{rr} is the intermediate principal stress and strike-slip faults result. They form in conjugate sets at angles of about 30° to the direction of maximum compressive stress; hence they trend roughly N 60°E and N 60°W.

3. Polar zones of normal faults. $\sigma_{rr} > \sigma_{\varphi\varphi} > \sigma_{\theta\theta}$. When both $\sigma_{\varphi\varphi}$ and $\sigma_{\theta\theta}$ become tensional σ_{rr} is the maximum principal stress, thus leading to normal faulting. The intermediate principal stress is $\sigma_{\varphi\varphi}$ so that the faults trend east–west. In the immediate vicinity of the poles $\sigma_{\varphi\varphi}$ and $\sigma_{\theta\theta}$ are nearly equal, so that the trends of the faults may not be strongly controlled.

These classifications have been used in Fig. 3 to interpret the stress patterns described there in terms of their tectonic implications. The addition of varying degrees of expansion or contraction of the planet can alter these relations. Thus, if a planet expands sufficiently, $\sigma_{\varphi\varphi}$ and $\sigma_{\theta\theta}$ may become tensional everywhere, extending the polar zone of normal faults until it covers the entire planet. Conversely, sufficient contraction may cause $\sigma_{\varphi\varphi}$ and $\sigma_{\theta\theta}$ to be everywhere compressional, thus extending thrust faulting over the entire planet. Figure 5 illustrates the effect of intermediate degrees of expansion or contraction on planets with both thick and thin lithospheric shells.

The above relations between faulting and stress are strictly valid only when all of the principal stresses are compressive. This always occurs at some depth below the surface, since a stress which is tensional at the surface becomes compressional at sufficient depth due to the addition of lithostatic pressure, although it remains smaller than the lithostatic pressure. However, the despinning model predicts that

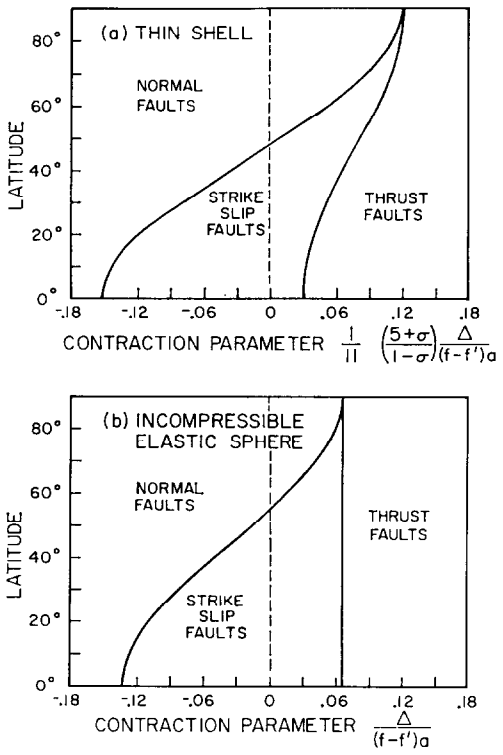

FIG. 5. The extent of the three tectonic provinces on a despun planet is plotted versus a parameter which describes the amount of contraction or expansion of the planet relative to its total change in flattening. Δ is the change in radius of the planet (positive for contraction), so Δ/a is the fractional contraction. $f - f'$ is the change in flattening of the planet. If no contraction takes place, the contraction parameter $\Delta/a(f - f') = 0$. In this case, strike-slip faulting extends to 48° with normal faults occurring poleward of this for a thin lithosphere (a). On an elastic sphere (b) this transition latitude is 55°. Contraction shifts the transition between strike-slip faulting and normal faulting poleward and eventually results in thrust faults which cover the entire surface of the planet. Sufficient expansion can cause normal faults to cover the entire planet. The horizontal scales in the two plots are arranged so that they are equal when $\sigma = \frac{1}{2}$.

rather large tensional stresses can develop near the surface. Since we are interested in surface tectonics, we must inquire into how these stresses affect the fault pattern. Brace (1964) has shown that intact rock specimens have very low tensional strengths. Several hundred bars is typical. When such specimens fracture, the fracture plane is either perpendicular to or forms a low angle with the axis of tension. There is a continuous transition between shear fractures making about a 60° angle with the minimum compressive stress axis and tensional fractures at 90° to the tensional stress axis. This transition occurs over a range of minimum principal stress of a few hundred bars. If this phenomenon is relevant to the crust of a despun planet, then we expect a gradual transition between the N 60°E and N 60°W strike-slip faulting province and the east–west-trending normal faults in the polar province.

On the other hand, the surface of a planet is unlikely to be as homogeneous and initially flawless as Brace's specimens were. It is more likely to be extensively fractured by meteorite impacts and igneous intrusions. The tensional strength of such material is effectively zero: it yields to tension by opening preexisting randomly oriented fractures. The stresses applied to the planet's crust are thus borne at greater depths where all stresses are compressive. When fractures occur at these deeper levels they propagate upward through the incoherent overburden. This argument supports the validity of Anderson's (1951) correlation between stress and tectonic pattern, despite the apparent occurrence of tensional stresses. The validity of Anderson's relations in the face of tensional stresses is further supported by model experiments in clay where tension was actually applied, and by Anderson's success in describing terrestrial geologic structures where similar complications arise (Billings, 1972). Thus, although the role of tensional stresses in the near-surface layers of the crust is somewhat obscure, field experience shows that Anderson's correlation between stress and tectonics is probably generally correct. We should nevertheless be aware that tensional fractures and joints may form part of the planetary lineament system. Where such

lineaments occur they will have dominant east–west trends.

Thus far, we have considered the lithosphere of the planet to be elastic. As the planet despins, elastic stresses build up. The maximum differences between principal stresses occur at the equator (where $\sigma_{\varphi\varphi} - \sigma_{\theta\theta}$ is the largest difference for strike-slip faulting and $\sigma_{rr} - \sigma_{\varphi\varphi}$ is the largest difference when thrust faulting occurs) and at the poles (where $\sigma_{rr} - \sigma_{\theta\theta}$ is maximum). When these stress differences exceed some critical value, which we shall call the lithospheric yield stress Y, failure occurs and faults form in orientations controlled by the elastic stress fields. Terrestrial experience indicates that this yield stress may be no more than a few hundred bars (Chinnery, 1964). As the planet despins still more, the regions of failure spread away from the poles and equator toward midlatitude regions. Eventually, the entire lithosphere may become faulted. The stresses in the faulted regions are not governed by elasticity. The stress equilibrium equations are still valid, but stress differences are held fixed at the yield point. The faulted regions are thus in a state of plastic equilibrium. In general, plastic equilibrium is very difficult to handle mathematically; however, if the lithosphere is thin the equations become simple, especially since our planet is axially symmetric. When the lithosphere is thick the situation is much more complex, and numerical solutions are necessary. We shall describe the analytical solutions for a thin lithosphere, since they qualitatively display all of the effects of plastic yielding.

The radial stress σ_{rr} in a thin lithosphere is smaller than the stresses $\sigma_{\theta\theta}$ and $\sigma_{\varphi\varphi}$ by a factor t/a. Thus, if Mercury had a 100-km-thick lithosphere, σ_{rr} would be about one-twentieth of $\sigma_{\theta\theta}$ or $\sigma_{\varphi\varphi}$. We can thus neglect σ_{rr} and $\sigma_{r\theta}$ to first order. The stress $\sigma_{\theta\varphi}$ is zero by axial symmetry, so that the stress equilibrium equations simplify to

$$\partial\sigma_{\theta\theta}/\partial\lambda + (\sigma_{\varphi\varphi} - \sigma_{\theta\theta}) \tan\lambda = 0. \quad (27)$$

There are three solutions to this equation corresponding to the three tectonic provinces:

1. Equatorial zone of thrust faulting. The difference between maximum and minimum principal stress is $\sigma_{\varphi\varphi} - \sigma_{rr} = Y$. But $\sigma_{rr} = 0$ so $\sigma_{\varphi\varphi} = Y$. Thus the plastic solution is

$$\begin{aligned} \sigma_{\theta\theta} &= Y - \text{constant}/\cos\lambda, \\ \sigma_{\varphi\varphi} &= Y. \end{aligned} \quad (28)$$

2. Equatorial to midlatitude zone of strike slip faults. In this zone the maximum difference is $\sigma_{\varphi\varphi} - \sigma_{\theta\theta} = Y$ and

$$\begin{aligned} \sigma_{\theta\theta} &= Y \ln(\cos\lambda) + \text{constant}, \\ \sigma_{\varphi\varphi} &= \sigma_{\theta\theta} + Y. \end{aligned} \quad (29)$$

3. Polar zone of normal faults. The maximum stress difference is $\sigma_{rr} - \sigma_{\theta\theta}$ in this zone, so that $\sigma_{\theta\theta} = -Y$ and

$$\begin{aligned} \sigma_{\theta\theta} &= -Y, \\ \sigma_{\varphi\varphi} &= -Y. \end{aligned} \quad (30)$$

Note that the addition of a hydrostatic stress field has no effect on these results, since none of the stress differences would be altered.

These plastic stress states preserve the same stress orientations as the elastic stress fields which produced them, so that the occurrence of faulting in a tectonic province does not change the character of the province. The only exception is in the equatorial province where any initial occurrence of thrust faulting is suppressed and replaced by strike-slip faulting as soon as strike-slip faulting begins elsewhere. Solutions (28) and (29) can be joined to give a zone of thrust faulting and strike-slip faulting only when strike-slip faulting extends poleward of 68°.4 latitude.

The plastic stress solutions in (28), (29), and (30) must be joined to the elastic

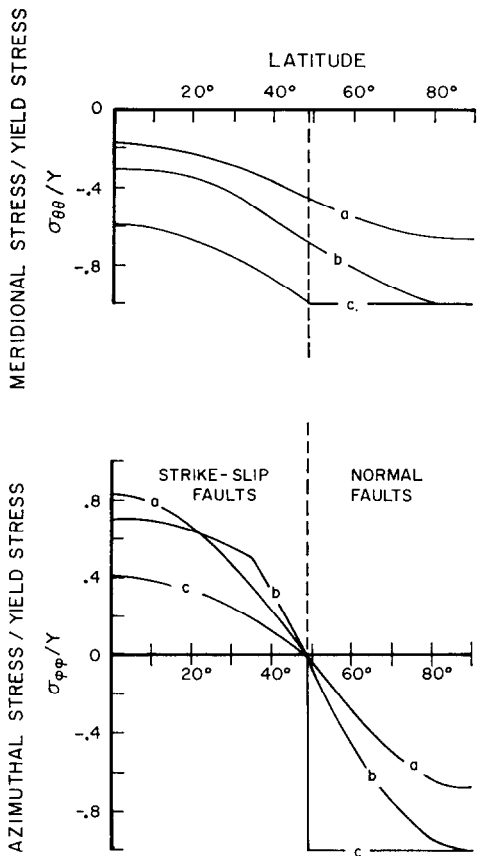

FIG. 6. Plastic yielding in a thin lithosphere begins at the equator when $\sigma_{\varphi\varphi} - \sigma_{\theta\theta} = Y$, the yield stress. Curves (a) show the stresses $\sigma_{\theta\theta}$ and $\sigma_{\varphi\varphi}$ when yielding has just begun. The elastic state is that appropriate for a despun planet with zero radial contraction or expansion. As the planet despins and stress increases, yielding in the strike-slip province spreads poleward to 35° latitude. At this time [curves (b)], yielding begins at the poles. Further despinning eventually brings the entire crust into the plastic state [curves (c)]. Strike-slip faults occur from 0 to 48° latitude and normal faults occur poleward of 48°. The boundary between these two regions is determined by the elastic stress field, and is maintained even in the fully plastic state.

solutions previously obtained. The boundary between the elastic and plastic regions always occurs at the latitude where the relevant stress difference reaches the yield point. This stress difference is smaller than the yield point in the elastic region, and is equal to it in the plastic region. In joining solutions from an elastic to a plastic region or from a plastic region to a plastic region, the only requirement is that $\sigma_{\theta\theta}$ be continuous. In particular, $\sigma_{\varphi\varphi}$ need *not* be continuous.

When the planet is sufficiently despun, the entire lithosphere enters the plastic state. Further despinning does not change the stress values given by (28), (29), and (30). Although the stresses remain constant, an arbitrary amount of strain may occur, so that the flattening decreases as the spin decreases. The entire stress field is specified by the condition that $\sigma_{\theta\theta}$ be continuous and by the constants in (28) and (29). These constants are determined solely by the latitudes at which one tectonic province transforms into another. Figure 6 illustrates the evolution of a thin lithosphere from an elastic to a fully plastic stress state. Curves (a) of the figure represent an elastic lithosphere in which failure has just begun at the equator. If the planet despins further, strike-slip failure spreads from the equator to 35° latitude, at which time normal faulting begins at the poles [curves (b)]. Curves (c) describe the stress field when the entire lithosphere has failed and become fully plastic. Further despinning of the planet does not alter the stress field; however, the amount of strain occurring in each province is unlimited. The latitude of the transition between strike-slip faulting and normal faulting is maintained even after the lithosphere becomes fully plastic. There is nothing in the *plastic* stress field which determines the transition latitude: this is established by the elastic field just before the lithosphere became fully plastic. The plastic lithosphere thus retains a memory of its previous elastic state. This result is characteristic of plasticity, owing to the highly nonlinear nature of the equations. Different plastic solutions may not be superposed.

The fact that the plastic state retains a memory of the previous elastic state does not mean that once the planet's lithosphere has become fully plastic the size of the tectonic provinces cannot change. If the elastic stress generated by each slight new loss of spin has the same pattern as the stress field which led to the fully plastic condition, the stress will be relaxed by the appropriate fault motion in each tectonic province. On the other hand, if the pattern differs (as may occur when the rates of despinning and radial contraction are not equal), the tectonic provinces will shift to accommodate the new stress.

The direction of this shift can be evaluated by a simple conceptual model. Suppose that some new combination of despinning and contraction tends to shift the tectonic provinces. Let the stress which would be generated in an elastic shell by some small increment of this combination of despinning and contraction be superposed on the plastic stress field in the crust. (Since real faults require more stress to initiate their motion than to continue it, this conceptual model may have a physical basis.) Evaluate the position of the new tectonic provinces by the usual arguments and then compute the plastic stress state according to these new boundaries. During this process portions of the lithosphere may even drop back into the elastic state. In this manner we proceed step by step in small increments until the desired total amount of despinning and contraction has occurred. It is evident that this method will drive the tectonic provinces in the same *direction* as that in which they would move if the stresses were purely elastic. The actual position of the provinces for a given amount of despinning and contraction could be much different than the elastic case, however. In particular, the equatorial thrust-faulting province is completely suppressed (and replaced by strike-slip faulting) until strike-slip faulting occurs poleward of 68°4.

We shall not further detail the evolution of a fully plastic lithosphere, since each possible history of despinning and contraction or expansion yields a different final state. The hysteresis in a plastic lithosphere means that these histories must be treated on a case-by-case basis. Moreover, the method we have described is based on an ideally plastic substance; a real lithosphere may tend to deform in the same style in which it had previously deformed, thus inhibiting the spread of tectonic provinces. This discussion of plasticity does, however, permit us to make some generalizations which are probably valid for a real planetary lithosphere. First, the tectonic pattern predicted by an elastic shell model is maintained even when the lithosphere becomes fully plastic (with the exception of the thrust faulting province). Changes in the tectonic pattern due to changes in the relative proportion of despinning and contraction are qualitatively predicted by the elastic model, although there is no quantitative comparison for a fully plastic lithosphere. The second major conclusion is that, despite the success of the elastic model in predicting the tectonic pattern, the numerical values of the stresses may be very different in elastic and plastic lithospheres. Clearly, stress differences in a plastic lithosphere can never exceed the yield point, while these differences are unlimited in an elastic lithosphere.

CONCLUSIONS

We have seen that despinning a planet with an elastic lithosphere produces a distinctive pattern of stress. The details of this stress pattern and the magnitudes of the stresses themselves depend most strongly upon the thickness of the lithosphere. The presence or absence of a dense core, and the compressibility of the elastic shell have only minor influences on the surface stress pattern. This *pattern* (although not the magnitude of the individual stresses) is

maintained even when the lithosphere fails and becomes fully plastic (except that thrust faulting is suppressed until strike-slip faulting occurs poleward of 68°.4 latitude). The size and character of the tectonic provinces defined by the surface stress patterns may be greatly altered if the planet contracts or expands slightly as it is despun. The one invariable feature of the great variety of tectonic patterns due to despinning plus contraction or expansion is that the azimuthal stress $\sigma_{\varphi\varphi}$ *always* exceeds the meridional stress $\sigma_{\theta\theta}$. A global system of fractures or lineaments in which this relation does not hold could not have been produced by despinning. We thus have one definitive test for rejecting the possibility that a given planetary lineament system is due to despinning. Another test, which may not be definitive, is to look for signs of tensional stresses in the polar regions. The existence of east–west-trending lineaments at high latitudes on a despun planet would provide further evidence that its lineament system was due to despinning. If the planet had contracted sufficiently as it despun these east–west lineaments could be absent, but only at the expense of north–south-trending thrust faults over most of the planet's surface.

The rich variety of tectonic patterns related to despinning and contraction or expansion suffers, at the moment, from the lack of an equally rich sample of despun planets. Mercury and the Moon are all we have to work with at the moment. The Mercurian lineament system is currently under study (Dzurisin, 1976), while the lunar lineament system has been given detailed study only on the basis of telescopic observations (Fielder, 1963; Strom, 1964). These observations indicate systems of NE- and NW-trending lineaments in the correct orientation for strike-slip faults with $\sigma_{\varphi\varphi} \gtrsim \sigma_{\theta\theta}$. The existence of a relatively strong NS trend is harder to reconcile with despinning. Future studies of the lineaments of the lunar farside and especially of the polar regions will be very useful in deciding whether or not despinning played a major role in creating the lineament systems. The lack of despun planets may be remedied in the future by spacecraft missions to photograph the surfaces of Titan and the Galilean satellites of Jupiter. These satellites are all large enough to provide excellent tests of whether or not despinning a planet can strongly influence its surface tectonics.

APPENDIX: CALCULATION OF STRESSES IN THE LITHOSPHERE OF A DESPUN PLANET

The geometry and definition of variables in the following discussion are given in Fig. 2. The general reasoning of the derivation is described in the text. We begin by computing the gravitational potentials and pressures in a hydrostatic planet which has a core with density ρ_c different from the lithosphere's density. The gravitational potential in the lithosphere for arbitrary flattening of the surface f and core f_i is

$$U_m = -\frac{\mu\kappa}{\rho_m}\left[\frac{3a^2 - r^2}{2a^2} + \frac{a}{r}(\eta - 1)\phi^3 + \frac{\Gamma}{3}\frac{r^2}{a^2}\right] + \frac{\mu\kappa}{\rho_m}\left[\frac{f}{10}\frac{r^2}{a^2} + \frac{f_i}{10}\frac{a^3}{r^3}(\eta - 1)\phi^5 + \frac{\Gamma}{12}\frac{r^2}{a^2}\right](1 - 3\cos 2\lambda), \quad \text{(A1)}$$

where we have defined the auxiliary quantities

$$\kappa = (4\pi/3)Ga^2\rho_m^2/\mu, \quad \text{(A2a)}$$

$$\Gamma = (3/4\pi)\omega^2/\rho_m G, \quad \text{(A2b)}$$

$$\phi = b/a, \quad \text{(A2c)}$$

$$\eta = \rho_c/\rho_m. \quad \text{(A2d)}$$

Note that when $\rho_c = \rho_m$ the quantity Γ in (A2b) is exactly the same as the m defined in the text [Eq. (4)]. The gravitational

potential in the core is

$$U_c = -\frac{\mu\kappa}{\rho_m}\left[\frac{3a^2 - r^2}{2a^2} + \frac{3b^2 - r^2}{2a^2}(\eta - 1) + \frac{\Gamma}{3}\frac{r^2}{a^2}\right] + \frac{\mu\kappa}{\rho_m}\left[\frac{f}{10}\frac{r^2}{a^2} + \frac{f_i}{10}\frac{r^2}{a^2}(\eta - 1) + \frac{\Gamma}{12}\frac{r^2}{a^2}\right](1 - 3\cos 2\lambda). \quad \text{(A3)}$$

The pressure in a hydrostatic sphere is given by $p = \text{const} - \rho U$ (when ρ is assumed constant). Since p (surface) $= 0$, we find that the pressure p_m in the lithosphere is

$$p_m = \mu\kappa\left[\frac{a^2 - r^2}{2a^2} + \frac{a - r}{r}(\eta - 1)\phi^3 + \frac{\Gamma}{3}\frac{r^2 - a^2}{a^2}\right] - \mu\kappa\left[\frac{f}{10}\frac{r^2}{a^2} + \frac{f_i}{10}\frac{a^3}{r^3}(\eta - 1)\phi^5 + \frac{\Gamma}{12}\frac{r^2}{a^2}\right] \times (1 - 3\cos 2\lambda). \quad \text{(A4)}$$

The pressure p_c in the core is

$$p_c = \mu\kappa\left[\frac{a^2 - \eta r^2}{2a^2} + \frac{(\eta - 1)}{2}\phi^2 + (\eta - 1)\phi^2\left(1 - \phi + \frac{\eta}{2}\frac{b^2 - r^2}{b^2}\right) - \frac{\Gamma}{3}\left(1 - \phi^2 + \eta\frac{b^2 - r^2}{a^2}\right)\right] - \mu\kappa\eta\left[\frac{f}{10}\frac{r^2}{a^2} + \frac{f_i}{10}\frac{r^2}{a^2}(\eta - 1) + \frac{\Gamma}{12}\frac{r^2}{a^2}\right] \times (1 - 3\cos 2\lambda), \quad \text{(A5)}$$

where the constant in p_c has been determined by requiring continuity of pressure across the core–lithosphere interface. The hydrostatic flattenings f and f_i are determined by requiring that the surfaces

$$r = a[1 - (f/6)(1 - 3\cos 2\lambda)], \quad \text{(A6a)}$$

$$r_i = b[1 - (f_i/6)(1 - 3\cos 2\lambda)] \quad \text{(A6b)}$$

are the equipotential surfaces of constant pressure. The resulting equations for f and f_i are

$$f = \frac{5}{6}\frac{\Gamma}{H - 1}, \quad \text{(A7a)}$$

$$f_i = \frac{5}{2}\frac{\Gamma}{(2\eta + 3)}\frac{H}{H - 1}, \quad \text{(A7b)}$$

where

$$H = \frac{5}{3}\frac{1 + (\eta - 1)\phi^3}{1 + \frac{3(\eta - 1)}{(2\eta + 3)}\phi^5}. \quad \text{(A8)}$$

We now suppose that the planet despins, decreasing Γ to Γ'. At the same time f decreases to f' and f_i to f_i'. The new values of flattening f' and f_i' will not, in general, correspond to hydrostatic values. In order to satisfy the surface boundary conditions

$$\sigma_{rr}\ (\text{surface}') = 0, \quad \sigma_{r\theta}\ (\text{surface}') = 0, \quad \text{(A9)}$$

and the core–lithosphere interface boundary conditions

$$\sigma_{rr}\ (\text{core}') = \text{constant}, \quad \sigma_{r\theta}\ (\text{core}') = 0, \quad \text{(A10)}$$

elastic strains must develop in the lithosphere. There are two types of elastic solutions. The homogeneous elastic solutions satisfy the equation (Jeffries, 1952)

$$\frac{\mu}{1 - 2\sigma}\nabla(\nabla\cdot\mathbf{u}) + \mu\nabla^2\mathbf{u} = 0, \quad \text{(A11)}$$

where $\mathbf{u}$ is the displacement of a point in the lithosphere,

$$\mathbf{u} = \mathbf{r} - \mathbf{r}'. \quad \text{(A12)}$$

There are also strains which develop in response to the change in gravitational potential due to the change in shape of the lithosphere. These strains must satisfy the inhomogeneous equation

$$[\mu/(1 - 2\sigma)]\nabla(\nabla\cdot\mathbf{u}) + \mu\nabla^2\mathbf{u} = -\rho_m\nabla(U_m' - U_m). \quad \text{(A13)}$$

TABLE AI

COEFFICIENTS OF THE ELASTIC SOLUTIONS TO (A11) AND (A13)

A. Homogenous solutions

	$n = 1$	$n = 3$	$n = -2$	$n = -4$
α	1	1	1	1
β	-3	$\frac{-7 + 4\sigma}{2\sigma}$	$-6\left(\frac{1 - 2\sigma}{5 - 4\sigma}\right)$	2

B. Inhomogenous solutions.

$U_m' - U_m = (c_2 r^2 + c_{-3} r^{-3})(1 - 3\cos 2\lambda)$

	$n = 3$	$n = -2$
α	$-\frac{\rho_m c_2}{28\mu}\left(\frac{1 - 2\sigma}{1 - \sigma}\right)$	$-\frac{\rho_m c_{-3}}{48\mu}\left(\frac{1 - 2\sigma}{1 - \sigma}\right)$
β	$+\frac{3\rho_m c_2}{56\mu}\left(\frac{1 - 2\sigma}{1 - \sigma}\right)$	$-\frac{\rho_m c_{-3}}{8\mu}\left(\frac{1 - 2\sigma}{1 - \sigma}\right)$

There are four solutions to (A11) and two solutions to (A13) for second-degree harmonic potentials acting on an elastic shell. These solutions are given by the general form

$$u_r = \alpha r^n (1 - 3\cos 2\lambda), \quad \text{(A14a)}$$

$$u_\theta = \beta r^n \sin 2\lambda, \quad \text{(A14b)}$$

$$u_\varphi = 0, \quad \text{(A14c)}$$

in terms of which the stresses are

$$\sigma_{rr} = \frac{2\mu r^{n-1}}{1 - 2\sigma}\{[(1 - \sigma)n + 2\sigma]\alpha + \sigma\beta\} \times (1 - 3\cos 2\lambda), \quad \text{(A15a)}$$

$$\sigma_{\theta\theta} = \frac{2\mu r^{n-1}}{1 - 2\sigma}\{[(1 + n\sigma)\alpha + \sigma\beta] - [3(1 + n\sigma)\alpha + (2 - \sigma)\beta] \times \cos 2\lambda\}, \quad \text{(A15b)}$$

$$\sigma_{\varphi\varphi} = \frac{2\mu r^{n-1}}{1 - 2\sigma}\{[(1 + n\sigma)\alpha + (1 - \sigma)\beta] - [3(1 + n\sigma)\alpha + (1 + \sigma)\beta] \times \cos 2\lambda\}, \quad \text{(A15c)}$$

$$\sigma_{r\theta} = 2\mu r^{n-1}\left(\frac{n - 1}{2}\beta - 3\alpha\right) \times \sin 2\lambda. \quad \text{(A15d)}$$

Solutions exist for $n = 1, 3, -2$, and -4. The relative magnitudes of α and β are given in Table AI for each of these solutions. The values of α and β for the inhomogeneous solutions corresponding to $n = 3$ and -2 are also given for a potential of the form

$$U_m' - U_m = (c_2 r^2 + c_{-3} r^{-3})(1 - 3\cos 2\lambda), \quad \text{(A16)}$$

where the constants c_2 and c_{-3} are obtained from an evaluation of $U_m' - U_m$ as deduced from (A1):

$$c_2 = -\frac{\mu\kappa}{\rho_m a^2}\left(\frac{f - f'}{10} + \frac{\Gamma - \Gamma'}{12}\right), \quad \text{(A17)}$$

$$c_{-3} = -\frac{\mu\kappa a^3}{\rho_m}(\eta - 1)\frac{f_i - f_i'}{10}\phi^5. \quad \text{(A18)}$$

The boundary conditions (A9) and (A10) require that

$$0 = p_m(\text{surface}') + \sigma_{rr}^{\text{inhomo}}(\text{surface}') + \sigma_{rr}^{\text{homo}}(\text{surface}'),$$
$$0 = \sigma_{r\theta}^{\text{inhomo}}(\text{surface}') + \sigma_{r\theta}^{\text{homo}}(\text{surface}'), \quad \text{(A19)}$$

and

$$0 = p_m(\text{core}') - p_c(\text{core}') + \sigma_{rr}^{\text{inhomo}}(\text{core}') + \sigma_{rr}^{\text{homo}}(\text{core}'), \quad \text{(A20)}$$
$$0 = \sigma_{r\theta}^{\text{inhomo}}(\text{core}') + \sigma_{r\theta}^{\text{homo}}(\text{core}'),$$

where p_m is the pressure in the lithosphere of the hydrostatic planet (A4) which must be evaluated on the new surface

$$r' = a[1 - (f'/6)(1 - 3\cos 2\lambda)]. \quad \text{(A21)}$$

Thus,

$$p_m(\text{surface}') = -(\mu\kappa/6)[1 + (\eta - 1)\phi^3] \times (f - f')(1 - 3\cos 2\lambda). \quad \text{(A22)}$$

Now $p_m - p_c$ must be evaluated at the base of the lithosphere (at the core–lithosphere interface), given by

$$r_i' = b[1 - (f_i'/6)(1 - 3\cos 2\lambda)] \quad \text{(A23)}$$

TABLE AII

ELEMENTS OF THE MATRIX EQUATION DETERMINING THE FOUR HOMOGENOUS ELASTIC SOLUTIONS FOR STRESS IN THE LITHOSPHERE OF A DESPUN PLANET

Equation

$$\begin{bmatrix} M_{11} & M_{12} & M_{13} & M_{14} \\ M_{21} & M_{22} & M_{23} & M_{24} \\ M_{31} & M_{32} & M_{33} & M_{34} \\ M_{41} & M_{42} & M_{43} & M_{44} \end{bmatrix} \begin{bmatrix} \alpha_1 \\ \alpha_2 a^3 \\ \alpha_3 a^{-2} \\ \alpha_4 a^{-4} \end{bmatrix} = \begin{bmatrix} K_1 \\ K_2 \\ K_3 \\ K_4 \end{bmatrix}$$

Matrix elements

$$M_{11} = -2 + 6(A_1 + B_1\phi^5)$$

$$M_{12} = 1 + 6(A_1 + B_1\phi^7)$$

$$M_{13} = 4\left(\frac{5-\sigma}{5-4\sigma}\right) + 6(A_1 + B_1\phi^2)$$

$$M_{14} = 8 + 6(A_1 + B_1)$$

$$M_{21} = -2 + 6(A_2 + B_2\phi^2)$$

$$M_{22} = \phi^2 + 6(A_2 + B_2\phi^4)$$

$$M_{23} = 4\left(\frac{5-\sigma}{5-4\sigma}\right)\frac{1}{\phi^3} + 6(A_2 + B_2/\phi)$$

$$M_{24} = 8/\phi^5 + 6(A_2 + B_2/\phi^3)$$

$$M_{31} = 6 + 6(D_1 + E_1\phi^5)$$

$$M_{32} = \frac{7+2\sigma}{\sigma} + 6(D_1 + E_1\phi^7)$$

$$M_{33} = 12\left(\frac{1+\sigma}{5-4\sigma}\right) + 6(D_1 + E_1\phi^2)$$

$$M_{34} = 16 + 6(D_1 + E_1)$$

$$M_{41} = 6 + 6(D_2 + E_2\phi^2)$$

$$M_{42} = \left(\frac{7+2\sigma}{\sigma}\right)\phi^2 + 6(D_2 + E_2\phi^4)$$

$$M_{43} = 12\left(\frac{1+\sigma}{5-4\sigma}\right)\frac{1}{\phi^3} + 6(D_2 + E_2/\phi)$$

$$M_{44} = 16/\phi^5 + 6(D_2 + E_2/\phi^3)$$

Auxiliary quantities

$$A_1 = \kappa\left[\frac{1}{70}\left(\frac{6-5\sigma}{1-\sigma}\right) - \frac{(1+(\eta-1)\phi^3)}{6}\right]$$

$$A_2 = \kappa\left[\frac{1}{7}\left(\frac{6-5\sigma}{1-\sigma}\right) - \eta\right]\frac{\phi^2}{10}$$

$$B_1 = \kappa\frac{\eta-1}{30}\left(\frac{5\sigma-1}{1-\sigma}\right)$$

$$B_2 = \kappa\frac{\eta-1}{30}\left[\frac{1}{2}\left(\frac{5\sigma-1}{1-\sigma}\right) + \eta\right]$$

$$D_1 = -\kappa\frac{9}{70}\left(\frac{1-2\sigma}{1-\sigma}\right)$$

$$D_2 = D_1\phi^2$$

$$E_1 = -\kappa\frac{\eta-1}{5}\left(\frac{1-2\sigma}{1-\sigma}\right)$$

$$E_2 = E_1$$

$$K_1 = \frac{\kappa}{84}\left(\frac{6-5\sigma}{1-\sigma}\right)(\Gamma - \Gamma')$$

$$K_2 = \frac{\kappa}{12}\left[\frac{1}{7}\left(\frac{6-5\sigma}{1-\sigma}\right) - \eta\right]\phi^2(\Gamma - \Gamma')$$

$$K_3 = \frac{-3\kappa}{28}\left(\frac{1-2\sigma}{1-\sigma}\right)(\Gamma - \Gamma')$$

$$K_4 = K_3\phi^2$$

so that

$$p_m(\text{core}') - p_c(\text{core}') = (\mu\kappa/6)\eta(\eta-1)\phi^2(f_i - f_i'). \quad \text{(A24)}$$

The inhomogeneous terms $\sigma_{rr}^{\text{inhomo}}$ and $\sigma_{r\theta}^{\text{inhomo}}$ must be functions of $U_m' - U_m$ and thus of $f - f'$ and $f_i - f_i'$. The boundary conditions (A19) and (A20) re-

duce to the simple case found in the text (14b), when Poisson's ratio $\sigma = \frac{1}{2}$. In this case $\sigma_{rr}^{\text{inhomo}}$ is simply the hydrostatic pressure due to $U_m' - U_m$ so that $p_m(\text{surface}') + \sigma_{rr}^{\text{inhomo}}(\text{surface}') = p_m'(\text{surface}')$, and $\sigma_{r\theta}^{\text{inhomo}} = 0$. In the general case of $\sigma \neq \frac{1}{2}$, (A19) and (A20) must be used.

The magnitudes of the four homogeneous solutions have not yet been specified. Equations (A19) and (A20) constitute four equations in six unknowns. The unknowns are $f - f'$, $f_i - f_i'$, and the magnitudes α_i ($i = 1, 4$) of the homogeneous solutions. Equations (A12) and (A14a) give us two more equations; at the surface (A6a) and (A21) imply

$$\begin{aligned} u_r(a) &= r - r' \\ &= -\tfrac{1}{6}(f - f')(1 - 3\cos 2\lambda) \\ &= (\alpha_1 + \alpha_2 a^3 + \alpha_3 a^{-2} + \alpha_4 a^{-4}) \\ &\qquad \times (1 - 3\cos 2\lambda); \end{aligned} \tag{A25}$$

thus,

$$f - f' = -6(\alpha_1 + \alpha_2 a^3 + \alpha_3 a^{-2} + \alpha_4 a^{-4}). \tag{A26}$$

At the core–lithosphere boundary (A6b) and (A23) give

$$\begin{aligned} u_r(b) &= r_i - r_i' = -\tfrac{1}{6}(f_i - f_i') \\ &\qquad \times (1 - 3\cos 2\lambda) \\ &= (\alpha_1 + \alpha_2 b^3 + \alpha_3 b^{-2} + \alpha_4 b^{-4}) \\ &\qquad \times (1 - 3\cos 2\lambda); \end{aligned} \tag{A27}$$

hence

$$f_i - f_i' = -6(\alpha_1 + \alpha_2 b^3 + \alpha_3 b^{-2} + \alpha_4 b^{-4}). \tag{A28}$$

The relations (A26) and (A28) allow us to replace $f - f'$ and $f_i - f_i'$ by expressions involving the four unknown α_i. Equations (A19) and (A20) thus become four equations for the four unknown α_i. The α_i can then be computed by standard matrix methods for given values of κ, Γ, ϕ, and η. The α_i are determined from an equation of the form

$$\begin{bmatrix} & & & \\ & M_{ij} & & \\ & & & \end{bmatrix} \begin{bmatrix} \alpha_1 \\ \alpha_2 a^3 \\ \alpha_3 a^{-2} \\ \alpha_4 a^{-4} \end{bmatrix} = \begin{bmatrix} K_1 \\ K_2 \\ K_3 \\ K_4 \end{bmatrix}. \tag{A29}$$

The matrix elements M_{ij} and constants K_i are given in Table AII. Once the α_i are found by inverting the matrix M, the stresses $\sigma_{\theta\theta}$ and $\sigma_{\varphi\varphi}$ can be computed. In particular,

$$\begin{aligned} \sigma_{\theta\theta}(\text{surface}') &= p_m(\text{surface}') \\ &\quad + \sigma_{\theta\theta}^{\text{inhomo}}(\text{surface}') \\ &\quad + \sigma_{\theta\theta}^{\text{homo}}(\text{surface}'), \end{aligned} \tag{A30a}$$

$$\begin{aligned} \sigma_{\varphi\varphi}(\text{surface}') &= p_m(\text{surface}') \\ &\quad + \sigma_{\varphi\varphi}^{\text{inhomo}}(\text{surface}') \\ &\quad + \sigma_{\varphi\varphi}^{\text{homo}}(\text{surface}'). \end{aligned} \tag{A30b}$$

The plots of $\sigma_{\theta\theta}$ and $\sigma_{\varphi\varphi}$ in the text of this paper were computed in the manner here described. A useful scaling relation for these stresses is that they are proportional to $(\Gamma - \Gamma')$, all other variables being the same.

ACKNOWLEDGMENTS

Dan Dzurisin's study of Mercurian lineaments provided the rationale for this study, and frequent discussions with him have sharpened my understanding of the kinds of predictions which are likely to be useful for photogeological work. I would also like to thank the Los Angeles County Superior Court for providing office space during part of this investigation.

REFERENCES

ANDERSON, E. M. (1951). *The Dynamics of Faulting.* Oliver and Boyd, Edinburgh.

BADGLEY, P. C. (1965). *Structural and Tectonic Principles.* Harper and Row, New York.

BILLINGS, M. P. (1972). *Structural Geology,* Prentice–Hall, Englewood Cliffs, N. J.

BINDER, A. B., AND MCCARTHY, D. W. (1972). Mars: The lineament system. *Science* **176,** 279–281.

BRACE, W. F. (1964). Brittle fracture of rocks. In *The State of Stress in the Earth's Crust* (W. R. Judd, Ed.), pp. 111–178. American Elsevier, New York.

BURNS, J. A. (1976). Consequences of the tidal slowing of Mercury. *Icarus* **28,** 453–458.

CHINNERY, M. A. (1964). The strength of the Earth's crust under horizontal shear stress, *J. Geophys. Res.* **69**, 2085–2089.

DZURISIN, D. (1976). Ph.D. Thesis, California Institute of Technology.

FIELDER, G. (1963). Lunar tectonics. *Quart. J. Geol. Soc. London* **119**, 65–94.

HANDIN, J. A. (1966). Strength and ductility. *Geol. Soc. Amer. Memoir* **97**, 223–289.

HOWARD, H. T., TYLER, G. L., ESPOSITO, P. B., ANDERSON, J. D., REASENBERG, R. D., SHAPIRO, I. I., FJELDBO, G., KLIORE, A. J., LEVY, G. S., BRUNN, D. L., DICKINSON, R., EDELSON, R. E., MARTIN, W. L., POSTAL, R. B., SEIDEL, B., SESPLAUKIS, T. T., SHIRLEY, D. L., STELZRIED, C. T., SWEETNAM, D. N., WOOD, G. E., AND ZYGIELBAUM, A. I. (1974). Mercury: Results on mass, radius, ionosphere and atmosphere from Mariner-10 dual-frequency radio signals. *Science* **185**, 179–180.

JEFFREYS, H. (1952). *The Earth*, 3rd ed. Cambridge Univ. Press, London/New York.

STONELEY, R. (1924). The shrinkage of the Earth's crust through diminishing rotation. *Mon. Not. Roy. Astron. Soc., Geophys. Suppl.* **1**, 149–155.

STROM, R. G. (1964). Analysis of lunar lineaments. I. Tectonic maps of the Moon. *Commun. Lunar Planetary Lab*, **2**, 205–216.

STROM, R. G., TRASK, N. J., AND GUEST, J. E. (1975) Tectonism and volcanism on Mercury, *J. Geophys. Res.* **80**, 2478–2507.

VENING-MEINESZ, F. A. (1947). Shear patterns of the Earth's crust. *Trans. Amer. Geophys. Union* **28**, 1–61.